Article

Journal of
Nanoscience and Nanotechnology
Vol. 17, 6367–6376, 2017
www.aspbs.com/jnn

Effect of Particle Size and Pyrite Oxidation on the Sorption of Gold Nanoparticles on the Surface of Pyrite

Yuhong Fu[1,2], Xin Nie[1], Zonghua Qin[1], Shanshan Li[3], and Quan Wan[1,*]

[1] State Key Laboratory of Ore Deposit Geochemistry, Institute of Geochemistry, Chinese Academy of Sciences, Guiyang 550081, China
[2] University of Chinese Academy of Sciences, Beijing 100049, China
[3] School of Chemistry and Materials Science, Guizhou Normal University, Guiyang, Guizhou 550001, China

The sorption of gold nanopartilces (AuNPs) with diameters of 16 or 39 nm on the surface of pyrite (80–100 or 140–160 mesh) was experimentally studied by systematically evaluating the effects of atmosphere, pH, reaction time and particle sizes on the sorption behavior. We have found that oxidation of pyrite plays a critical role in the sorption process, which increases the pH_{iep} of pyrite to 4–5 and decreases the pH of the suspension. The presence of citrate and AuNPs does not seem to significantly change the pyrite oxidation pathway. A smaller particle size of pyrite and aerobic atmosphere accelerates the overall oxidation rate. Under suitable conditions, the negatively charged AuNPs can be adsorbed onto positively charged surface of oxidized pyrite through electrostatic attraction. A complete sorption of AuNPs was observed at pH < 3 after two days of pyrite oxidation. The initially alkaline conditions (pH 10) appear to promote the pyrite oxidation, and the resulting oxidized colloidal particles (iron oxide or hydroxide) could adsorb or destabilize AuNPs due to heteroaggregation. Our experimental findings suggest that surface charge property and reaction conditions are crucial in determining the migration and distribution of nanoparticles in the natural environment, which may improve our understanding of mineralization mechanisms of "invisible gold" and the potential fate of AuNPs in aquatic environments.

Keywords: Gold, Nanoparticles, Pyrite, Oxidation, Sorption, pH.

1. INTRODUCTION

Nano- and submicron-sized gold particles are increasingly recognized as an important component of certain hypogene and secondary ore deposits.[1–4] For example, in the Carlin-type deposits, transmission electron microscopy (TEM) demonstrates that gold nanoparticles (AuNPs) with a diameter of 5–10 nm are closely associated with the iron sulfides of the ore samples,[3,4] and by estimation up to ~8% of Au may exist in the form of metallic nanoparticles.[1] AuNPs were also identified in some weathering-related supergene deposits.[2,5–7] As an integral effort to understand the corresponding metallogenesis, extensive research work has been devoted to the investigation of the occurrence state of Au, which includes the structures, morphology and properties of the Au species.[4,8–12] Meanwhile, three processes were envisioned for the formation of AuNPs in sulfides:[3,4,13] (1) exsolution from a metastable arsenian pyrite matrix during evolution of the deposit; (2) direct deposition or sorption into pyrite from a hydrothermal fluid; (3) dissolution-reprecipitaion and/or replacement reaction. However, until now, a commonly accepted mechanism for the genesis of AuNPs and their associated nanosize effect on the ore-forming process are still unknown.

Owing to their stability and transportability, colloidal particles may play a significant role in the formation of some hydrothermal ore deposits.[13–15] Although controversy still exists regarding whether AuNP is a form of transportation of gold or a metallogenic product,[16,17] the migration and deposition of AuNPs is quite arguably involved as an essential step in the metallogenic process. Firstly, AuNPs are fairly stable under the temperature and pressure conditions of the ore-forming fluids for the Carlin-type deposits (i.e., $T < 300$ °C, $P < 60$ Mpa).[18] Evidence indicated that native AuNPs (mean diameter ~4 nm) in pyrite from a Carlin-type deposit could remain stable at up to 370 °C, whereas at higher temperatures, AuNPs coarsened because of solid-state Ostwald ripening.[11] AuNPs (~30 nm) showed a higher stiffness than bulk gold, and

*Author to whom correspondence should be addressed.

neither phase transformation nor noncubic lattice distortions were detected at 30 GPa.[19] When AuNPs (10–20 nm) were pressurized up to 71 GPa, their diameter remained at nanometer scale (~5 nm).[20] Secondly, even in the case that high valence Au(I or III) complexes instead of AuNPs may be the dominant transportation form, the local environment of the host rock containing reductive matters (e.g., organic or pyrite) should facilitate the formation of AuNPs, and subsequent remobilization and migration of AuNPs is still highly possible. Consistently, several studies suggested that gold might migrate in the form of Au colloid during the ore-forming process.[14, 15, 21–23] For example, colloidal transportation and deposition of gold and silica in Sleeper deposit of Nevada were suggested through textural evidences.[15] Since understanding the gold deposition process and mechanism is of great importance to revealing the metallogenesis of these ore deposits, the sorption of gold on sulfide minerals has received extensive attention in recent years. However, most research focused on the interaction between high valence Au species and sulfide minerals, and found that gold could form metallic nanoparticles or Au(I) could bond with sulfur on the mineral surface.[24–29] Despite the obvious role of AuNPs in the ore-forming process, studies on sorption of AuNPs on the surface of sulfide minerals were seldom referenced in literature.[30]

Pyrite is a very abundant sulfide mineral and was frequently found to be the major gold-bearing mineral. Surface properties of pyrite not only play a part in the formation of gold deposits and but also affect the mineral processing of gold ores.[31, 32] Pyrite is easily oxidized when exposed to air and water.[33–35] Even in the absence of oxygen and other oxidants, pyrite in aqueous environment may be oxidized and the corresponding oxidation products (Fe^{2+} and SO_4^{2-}) can be detected in 10 hours.[36] Among the oxidation products of pyrite, iron oxides and iron (hydr)oxide were found to adsorb natural AuNPs in supergene deposits.[6, 7] Besides, auriferous sulfide mineral oxidation may result in the redistribution of gold.[37, 38] Although interaction between pyrite and Au species was often studied, experimental complications could arise due to pyrite oxidation. For example, previous studies have shown that the amount and rate of high valence gold sorption on pyrite can be significantly affected by the degree of pyrite oxidation.[28, 32, 39, 40] However, to the best of our knowledge, the effect of pyrite oxidation on AuNPs-pyrite sorption has not been systemically studied.

We believe that experimental simulations of the deposition of nanoparticulate matters are of fundamental importance in elucidating many nanoparticle-related geological and geochemical processes, including the microscopic metallogenic mechanism of Carlin-type deposits. Thus we studied the sorption of AuNPs on pyrite under different pHs and atmospheres (Ar and air). Considering the size-dependent physical or chemical properties of AuNPs[41] and the fact that gold grade of natural ore samples is usually correlated with the size of pyrite,[9, 42, 43] we also assessed the size effect on AuNPs-pyrite sorption in the present study. Our experimental results revealed dominant roles of oxidation and surface charge of pyrite in the process of AuNP sorption. The findings will improve our understanding of metallogenic processes of Carlin-type deposits and the transport behaviors of nanoparticles in aquatic environments, and may provide new insight into mineral processing of "invisible" gold.

2. MATERIAL AND METHODS

2.1. Reagents

Chloroauric acid tetrahydrate ($HAuCl_4 \cdot 4H_2O$) (≥99.9%) was purchased from Shanghai Jiuyue Chemical Reagent Company, China. Sodium citrate dihydrate (≥99.0%) was purchased from Shanghai Shenbo Chemical Reagent Company, China. Hydrochloric acid (36~38%), nitric acid (65~68%) and ethanol (≥99.7%) were purchased from Sinopharm Chemical Reagent Company, China. Sodium hydroxide (>96%) was purchased from Chongqing Chuandong Chemical Reagent Company, China. All chemicals were of analytical or guaranteed reagent grade, and were used without further purification. Before use, all glassware and magnetic stir bars were thoroughly soaked in aqua regia (HCl/HNO_3 = 3:1, V/V), and then rinsed with copious amounts of deionized water. Deionized water was obtained from a Millipore synergy UV system (resistivity, 18.2 $M\Omega \cdot cm$).

2.2. Synthesis of Gold Colloid

AuNPs were synthesized using Frens method[44] and the particle sizes were controlled by changing the molar ratio of citrate/$HAuCl_4$. 10.5 or 3.6 mL of sodium citrate solution (1.00%, w/w) was quickly added to 300 mL of boiling $HAuCl_4$ solution (0.01%, w/w) and then stirred for 30 min. After the reaction mixtures changed to a wine-red color, the samples were cooled down to ambient temperature and stored in a fridge at 4 °C. The initial molar ratio of citrate/$HAuCl_4$ was 4.65 and 1.58 respectively. The morphology of AuNPs was characterized using a transmission electron microscope (TEM; JEM-2000FXII, JEOL, Japan) and the particle size was analyzed using the ImageJ (US National Institutes of Health) software. According to the size analysis results (described in Section 3.1), these two Au colloid samples were named as Au-16 and Au-39 (Au concentrations: 57.8 and 58.3 mg/L), respectively.

2.3. Pretreatment of Pyrite

Pyrite sample was collected from Meitan, Guizhou Province, China. After crushing, separation and cleaning, it contained ~43.4% iron and ~56.6% sulfur (w/w). The pyrite was then sieved into two size fractions (80–100 and 140–160 mesh, respectively). To remove any oxidation products and finer particles adsorbed on the mineral surface, hydrochloric acid cleaning and ultrasonic treatment

were performed by the method conducted by Descostes et al.[45] Scanning electron microscopy (SEM; JSM-6460LV, JEOL, Japan) was employed for morphological analysis. Elemental analysis was carried out by energy dispersive X-ray spectroscopy (EDS). The grain-sizes of 80–100 and 140–160 mesh pyrite were measured using a particle size analyzer (Mastersizer 2000, Malvern, UK), and the pyrite samples were named as Py-242 and Py-134 based on the test results (see Section 3.1).

2.4. Sorption Experiments

To study the size effect on sorption, AuNPs and pyrite with different sizes were used in the sorption experiments under ambient conditions. In a typical sorption experiment, 10 mL of suspension containing 0.5 g of pyrite (Py-134 or Py-242) and 10 mL of Au colloid (Au-16 or Au-39) were added into a 25 mL conical flask. The sorption suspensions were shaken in a thermostatic oscillator (150 rpm) throughout the experiment, and the temperature was maintained at approximately 25 ± 1 °C. The pHs of suspensions were measured at specified time intervals. Then, the suspensions were centrifuged for 30 min (Au-16 series at $100 \times$ g, Au-39 series at $50 \times$ g), and 2 mL of supernatants was digested (1 mL aqua regia, overnight) to analyze Au concentrations using a flame atomic absorption spectrophotometer (AAS; 990SUPER, Persee, China). A small fraction of the suspension (Au-16 + Py-134 pyrite) was characterized by TEM equipped with EDS.

Furthermore, we assessed the possible effects of AuNPs and citrate on pyrite oxidation. A batch of pyrite (Py-134, Py-242; 0.5 g) was added to 10 mL of Au colloid (Au-16), water, and sodium citrate solution, respectively. The concentration of sodium citrate for the oxidation experiments was 236.6 mg/L, which was compatible with the residual citrate concentration in the as-synthesized Au-16 colloid.[46] The samples were shaken at 25 °C for several days. Then, the pHs and Fe concentrations of the supernatants were measured using a pH meter and AAS, respectively.

The sorption processes of AuNPs on the pyrite surface under different atmospheres (normal air or anoxic condition) and pHs were systematically conducted to investigate the effect of pyrite oxidation on sorption. In each penicillin bottle, 0.5 g of pyrite (Py-242) was mixed with 10 mL of Au colloid (Au-16). By adding suitable amounts of HCl (2 mol/L) or NaOH (1 mol/L), the initial pHs were adjusted to 3.02, 6.11, 7.06 and 10.02, respectively. For the anoxic experiment, all bottles were put into a glove box, then vacuumed up and purged with argon for three cycles. The bottles were then firmly pressed with rubber stoppers and aluminum caps, before being taken out of the glove box and sealed with Parafilm M® (Bemis Company, Inc.). For the aerobic experiment, all the operations were carried out in the air, and a hole was pierced through the cap to keep the suspensions in contact with air. Considering that the alkaline suspensions would easily absorb CO_2 from air and cause a decline in pH, we did not conduct the aerobic sorption experiment for the sample with an initial pH of 10.02. After all the bottles were shaken at 25 °C for 12 days, the pyrite was separated by centrifugation ($100 \times$ g, 30 min) and supernatants were digested for measuring the Au and Fe concentrations by AAS. Meanwhile, pyrite-free Au colloids with matching initial pHs were used as control samples in the anoxic experiment.

3. RESULTS AND DISCUSSION

3.1. The Morphological and Size Characterizations of AuNPs and Pyrite

Most of our AuNPs were spherical in shape, except a small amount of ellipsoidal and pyramidal particles (Fig. 1(a)). The average diameter of Au-16 was ca. 16.4 nm based on the statistical analysis of more than 100 particles in the TEM images, and the relative standard deviation (RSD) was 12.5% (Fig. 1(b)). Unlike Au-16, most of AuNPs in Au-39 were ellipsoidal with a relatively wider size distribution (Fig. 1(c)). The average equivalent diameter of Au-39 was ca. 38.9 nm and RSD was 17.5% (Fig. 1(d)). Because of the difference in the initial citrate concentrations, which resulted in different pHs and possibly different reaction pathways, the extent of aggregation and anisotropic growth appeared significantly higher in Au-39.[47] Nevertheless, the surface structure of AuNPs with different sizes and shapes should be quite comparable due to the very similar synthetic method. The sieved pyrite displayed a satisfactory monodispersity in size, and the mean sizes of 80–100 (Py-242) and 140–160 mesh (Py-134) pyrites were 241.9 μm and 134.3 μm, respectively. After hydrochloric acid and ultrasonic cleaning, the pyrite surface appeared rather clean (see SEM and EDS results in Fig. 2) suggesting that the oxidation products and the adsorbed fine particles had been thoroughly removed.

3.2. The Size Effect on Sorption of AuNPs on Pyrite

Sorption experiments of AuNPs with different diameters (Au-16, Au-39) on pyrite with different sizes (Py-134, Py-242) under ambient conditions were conducted to study the size effect on sorption (Fig. 3). With the prolongation of time, the sorption percentages of AuNPs increased in pace with the decrease of the pH. When the sorption percentages reached 100%, the pH was lowered to about 2.90–3.00, and the pH decreased continually as the sorption time further increased owing to the oxidation of pyrite.

An apparent size dependence for the changes of pH and sorption percentages was revealed:

(1) Compared with Py-242 series, the pH decreased faster for the smaller pyrite (Py-134) series, and the overall sorption rate increased with the decrease of pyrite size (Fig. 3(a));

(2) The overall sorption rate in Au-39 series was much higher than that of Au-16 series (Fig. 3(b)).

It should be noted that these two Au colloids had different initial pHs (i.e., initial pH of 6.13 for Au-16 vs. 3.90

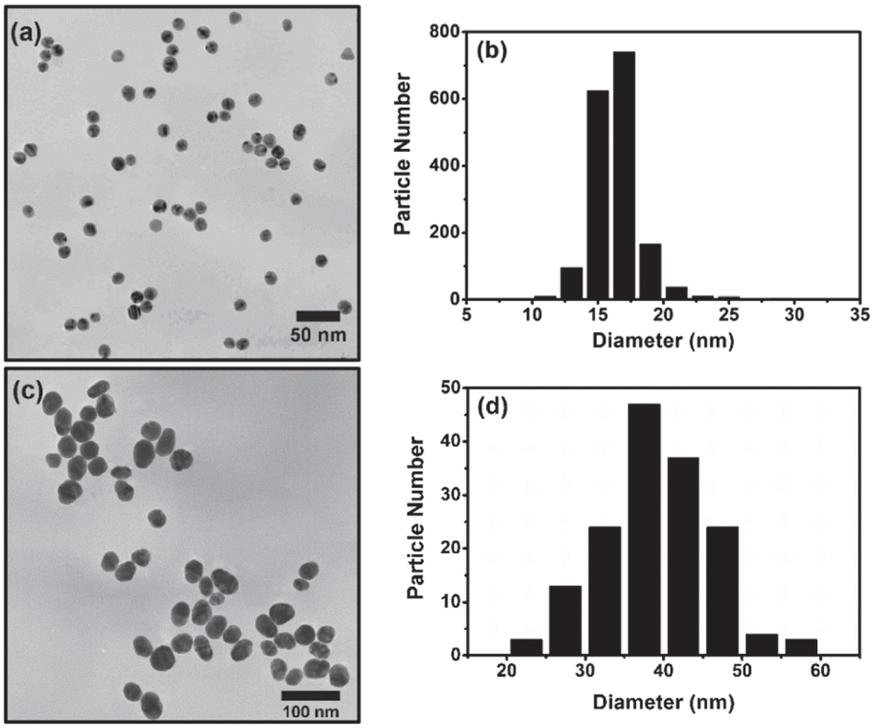

Figure 1. TEM micrographs and size distribution of AuNPs samples. (a, b) sample Au-16, and (c, d) sample Au-39.

for Au-39) due to the difference in citrate concentrations. After shaken for 9 days, a small fraction of a sorption suspension (Au-16 + Py-134; 100% sorption; pH 2.90) was taken for TEM observation (Fig. 4). The pyrite particles with a diameter of hundreds of micrometers were too large to observe the AuNPs-pyrite sorption using TEM. However, on edges of certain fragments of pyrite, spherical AuNPs with approximately the original size were found substantially distributed in the black region presented in Figures 4(a) and (b), and Au, Fe and S peaks were quite obvious in EDS (Fig. 4(c)). Therefore, we speculate that the surface of pyrite was completely covered with AuNPs by the strong adsorbing effect at the fragments of pyrite surface. As mentioned earlier, the above observed variation patterns of pH and sorption percentage with time and particle size are closely related to pyrite oxidation, which will be further discussed in the following sections.

3.3. Oxidation of Pyrite in the Presence of AuNPs and Citrate

When exposed to a small amount of water and oxygen, pyrite surface can be easily oxidized within several hours or minutes.[33, 34, 48] Oxidation of pyrite results in the generation of H^+, Fe^{2+}/Fe^{3+} and SO_4^{2-}, which is consistent with the observation that pH decreases with time in our sorption experiments. The oxidation of pyrite is a complicated process and it could be affected by many factors (e.g., pH, oxidant, size, composition, microorganism and clay mineral).[49–51] Despite considerable research efforts during the past decades, the exact mechanism of pyrite oxidation remains elusive.[33, 52] In aqueous systems, where the most important oxidants for pyrite oxidation are O_2 and Fe^{3+},[53] the overall oxidizing process of pyrite is usually expressed by reactions 1–4.[33, 54, 55] The oxidation of pyrite by O_2 is given by reactions 1 and 2 in acidic conditions and by reaction 3 in alkaline conditions, and the oxidation of pyrite by Fe^{3+} in acidic conditions is expressed by reaction 4.

$$2FeS_2(s) + 7O_2(g) + 2H_2O(l) = 2Fe^{2+}(aq) + 4SO_4^{2-}(aq) + 4H^+(aq) \quad (1)$$

$$4Fe^{2+}(aq) + O_2(g) + 4H^+(aq) = 4Fe^{3+}(aq) + 2H_2O(l) \quad (2)$$

$$4FeS_2(s) + 15O_2(g) + 14H_2O(aq) = 4Fe(OH)_3(s) + 8SO_4^{2-}(aq) + 16H^+(aq) \quad (3)$$

$$FeS_2(s) + 14Fe^{3+}(aq) + 8H_2O(l) = 15Fe^{2+}(aq) + 2SO_4^{2-}(aq) + 16H^+(aq) \quad (4)$$

In our experiments, pyrite oxidation happened in the presence of AuNPs and citrate, and consequently we need to verify whether this incurs a substantial impact on the oxidation process. Pyrite with different sizes (Py-134 and Py-242, 0.5 g) was added to 10 mL Au colloid (Au-16), deionized water or sodium citrate solution (236.6 mg/L), respectively. After shaking for a definite time, the pHs and Fe concentrations of the suspensions were measured

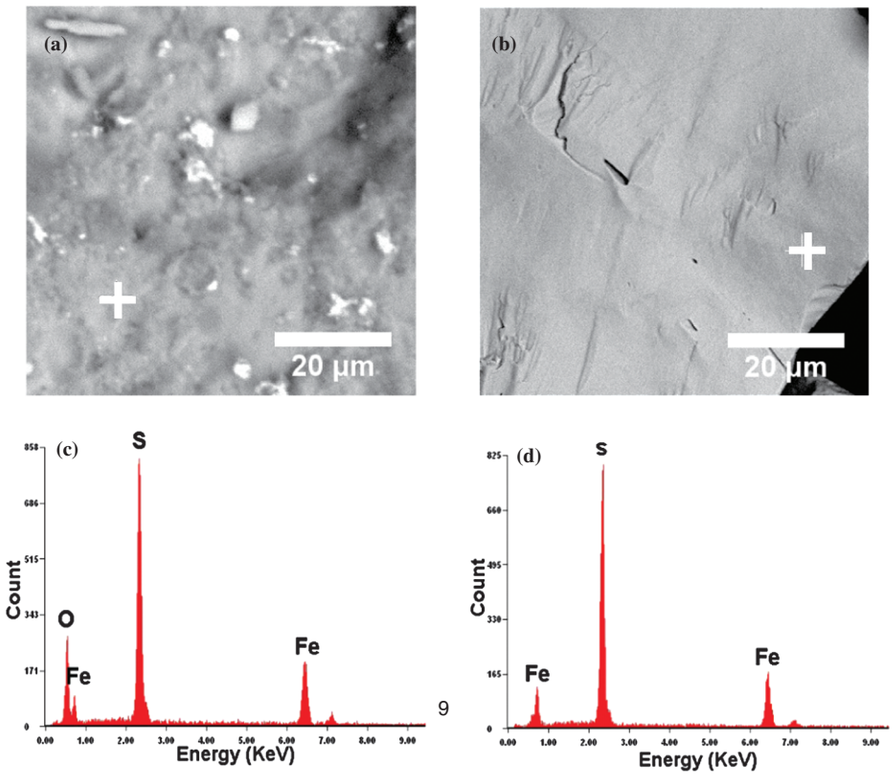

Figure 2. SEM images and EDS spectra of pyrite before and after hydrochloric acid and ultrasonic cleaning. (a) SEM image of pyrite before cleaning, (b) SEM image of pyrite after cleaning, (c) EDS spectrum of pyrite before cleaning (analysis point was shown as the cross in (a)), and (d) EDS spectrum of pyrite after cleaning (analysis point was shown as the cross in (b)).

(Fig. 5, Table I). Even though the reaction conditions (shaking time and mineral sizes) were quite different, the data points of samples containing citrate (Au colloid and citrate solution) all fall along a straight line with a correlation coefficient of 0.993. Similarly, there is a good linear relationship (correlation coefficient: 0.999) between H^+ and Fe concentrations in the samples of pyrite in water. The slope of each trend line in Figure 5 is approximately 1 (1.17 and 1.06, respectively), which agrees well with the molar ratio of the oxidation products H^+ and Fe^{3+} according to the oxidation reaction Eqs. (1) and (2). Additionally, we found that under otherwise similar conditions, the concentrations of H^+ and Fe increase with the shaking time, but decrease with pyrite particle size (Table I). After prolonged stirring time (e.g., 107 days), the Fe concentrations of samples (Py-242) were roughly the same regardless of whether the reaction media is in water or in citrate solution (Table I). All these results indicate that the presence of AuNPs or citrate does not significantly change the overall mechanism of pyrite oxidation. The difference in the intercepts of these two trend lines is mainly due to the weak alkalinity of citrate, which could consume certain amounts of H^+ during the process of pyrite oxidation.

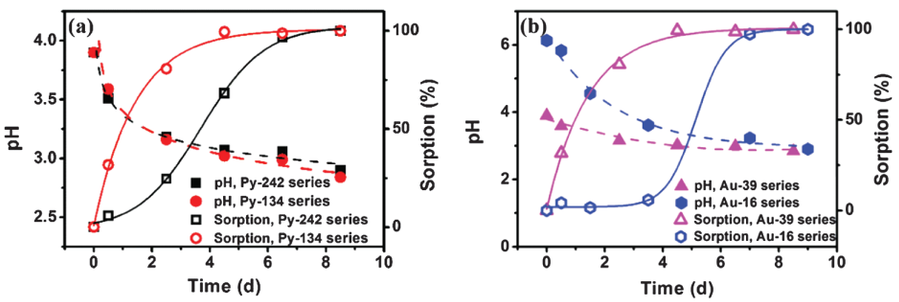

Figure 3. Changes of pH and sorption percentage of AuNPs on pyrite as a function of time (in air). (a) 0.5 g pyrite: Py-134, Py-242; 10 mL AuNPs: Au-39. (b) 0.5 g pyrite: Py-134; 10 mL AuNPs: Au-16, Au-39.

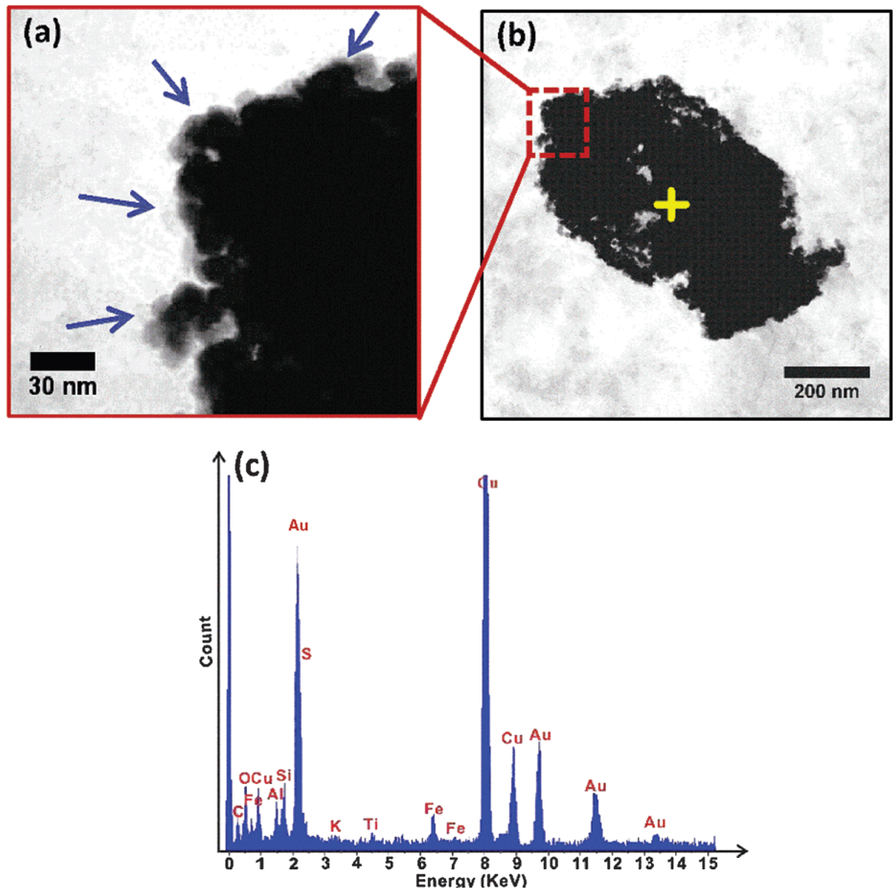

Figure 4. TEM images (a and b) and EDS (c) of a sorption sample (Au-16 + Py-134 pyrite, after shaking for 9 days in air). (a) The magnified TEM image recorded from the cubic area in (b) (arrows point at some AuNPs). (b) TEM micrograph of the AuNPs adsorbed on pyrite fragments (the black area). (c) EDS spectrum of the selected point in (b).

3.4. Effect of Pyrite Oxidation on Sorption of AuNPs

Although citrate and AuNPs have no significant effect on pyrite oxidation, the influence of pyrite oxidation on sorption of AuNPs cannot be ignored. It is well known that the change of chemical composition could lead to the alteration of surface charge density through dissociation of surface functional groups or adsorption of ions.[56] Therefore, to clarify whether compositional change (surficial or aqueous) caused by pyrite oxidation would affect the sorption of AuNPs, the sorption experiments of pyrite (Py-242)

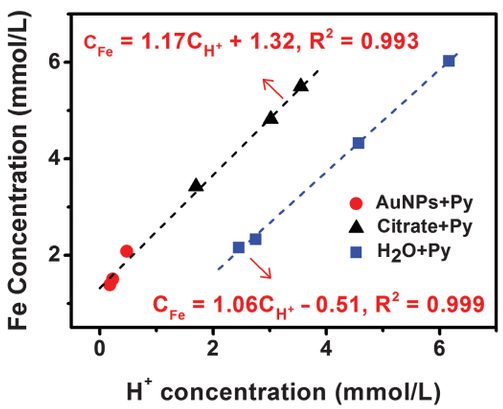

Figure 5. Linear relationship between concentrations of Fe and H^+ in the supernatants of the pyrite samples oxidized in H_2O, citrate or gold colloid under aerobic conditions (see Table I for details).

Table I. Concentrations of Fe and H^+ in supernatants of oxidized pyrite samples (in H_2O, citrate or gold colloid under aerobic conditions).

Pyrite	Reaction medium	Time (days)	C_{Fe} (mmol/L)	C_{H^+} (mmol/L)
Py-242	Colloid*	21	1.51	0.23
Py-242	Colloid*	21	1.39	0.18
Py-134	Colloid*	21	2.09	0.48
Py-242	H_2O	63	2.16	2.45
Py-134	H_2O	63	2.33	2.75
Py-242	H_2O	107	4.33	4.57
Py-134	H_2O	107	6.03	6.17
Py-242	Citrate**	97	3.43	1.70
Py-242	Citrate**	107	4.83	3.02
Py-134	Citrate**	107	5.50	3.55

Notes: *Au colloid: Au-16, **sodium citrate solution: 236.6 mg/L.

and AuNPs (Au-16) were performed under different atmospheres (air or Ar) and pHs (3–10). Since pyrite oxidation is accompanied by the increase of H^+ and Fe^{3+}/ Fe^{2+} concentrations (reaction 1–4), we simultaneously monitored the pHs and Fe concentrations along with Au concentrations in the sorption experiments.

Changes of the pHs for suspensions after shaking for 12 days were shown in Figure 6. The pHs of Au colloids (control samples without pyrite) remained unchanged under both acidic and neutral conditions. However, the pH of control samples declined under alkaline conditions (pH 10.02) possibly because of the absorption of CO_2 permeating through the caps of the penicillin bottles. The pHs of sorption samples (suspensions containing pyrite and Au colloids) in anoxic system decreased slightly, suggesting that the pyrite was partially oxidized even in anoxic experiments. Possible sources of oxygen might include dissolved oxygen from the aqueous solution in addition to the air diffusion though the bottle caps. In contrast, the pHs of samples in the aerobic experiment declined more evidently (e.g., initial pH of 7.06 declined to 3.20). In both anoxic and aerobic experiments, Fe concentrations increased with initial pH (Fig. 7), which was consistent with the experimental findings that oxidation rate of pyrite increased with pH.[33, 49, 51, 57, 58] The possible reason is that at higher pH, OH^- may be involved in an inner-sphere electron transfer process,[59, 60] in which an electron and an OH^- can be exchanged concurrently between pyrite and its surface oxidation products.[49] Besides, OH^- can neutralize the oxidation production of H^+, and thus accelerates the oxidation reaction. The Fe concentrations in aerobic system were much higher than that in anoxic system because the oxidation of pyrite in aerobic conditions is faster than that in anoxic conditions with much lower concentration of O_2.

Au concentrations of these three different reaction series (anoxic, aerobic experiments and references) after shaking for 12 days were significantly different (Fig. 8). For the pyrite-free references, Au concentration decreased slightly

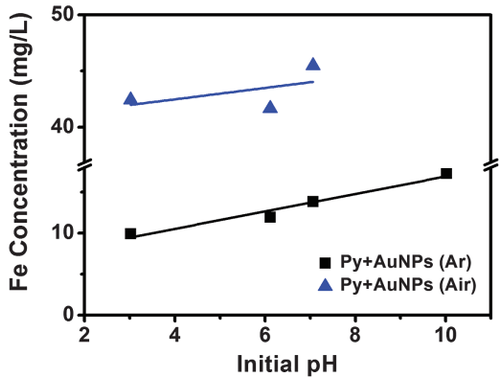

Figure 7. Fe concentrations in anoxic and aerobic samples (Au-16 + Py-242) after shaking for 12 days as a function of initial pH.

at initial pH 3.02, and a very small amount of black sheet agglomerates could be observed in the gold colloidal solution. This is ascribed to the partial neutralization of AuNPs by protonation of citrate ligand at lower pH which resulted in the decrease of electrostatic repulsion between AuNPs, and consequently reduced the stability of Au colloids.[61, 62] The changes of Au concentrations in references with initial pH ranging from 6.11 to 10.02 were almost negligible compared to the original level. However, there was an apparent initial pH dependence of Au sorption on pyrite in anoxic and aerobic experiments. When initial pH was 3.02, Au concentrations in the solution contained pyrite were about 0 in both anoxic and aerobic conditions, implying that the AuNPs might be adsorbed completely by pyrite. At initial pH of 6.11 and 7.06, Au concentrations of anoxic systems were essentially unchanged compared to the original Au concentration (57.8 mg/L). While in aerobic system, Au concentrations decreased significantly. At initial pH 10.02, Au concentration was reduced to 29.8 mg/L in anoxic system.

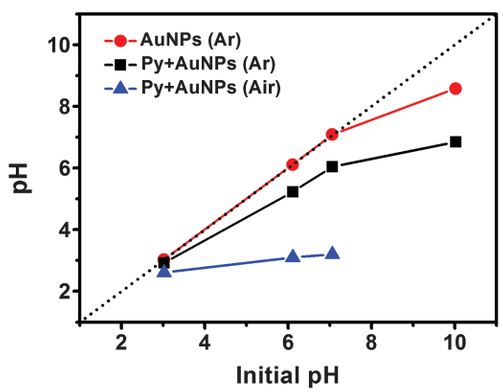

Figure 6. The pHs of three different reaction series: AuNPs references (Au-16), the anoxic system (Au-16 + Py-242) and the aerobic system (Au-16 + Py-242), after shaking for 12 days as a function of initial pH. Dotted line shows the 1:1 diagonal line.

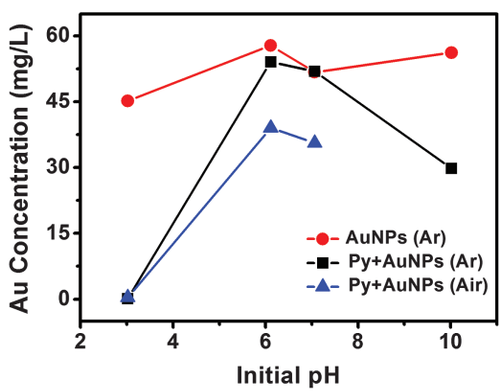

Figure 8. Au concentrations of three different reaction series: AuNPs references (Au-16), the anoxic system (Au-16 + Py-242) and the aerobic system (Au-16 + Py-242), after shaking for 12 days as a function of initial pH.

3.5. Sorption Mechanism

Based on the above results, we can reasonably deduce that oxidative condition, pH, and particle sizes (of AuNPs and pyrite) all play substantial roles in the process of AuNPs sorption on pyrite. We emphasize the importance of the electrostatic mechanism in the AuNPs-pyrite sorption process, and would first describe the basic model and then discuss how such a mechanism fits our experimental findings.

AuNPs synthesized via citrate reduction always carry negative charges due to citrate adsorption on the nanoparticle surface.[63–65] On the other hand, pristine pyrite (without any oxidation) has an isoelectric point (pH_{iep}) < 2,[66–68] which indicates that pyrite should be negatively charged at pH > 2 and would thus repel the negatively charged AuNPs under our experimental settings (pH 3–10). However, pyrite can be easily oxidized, and depending on the extent of oxidation, the isoelectric point of oxidized pyrite could shift higher (e.g., $pH_{iep} \geq 6$) as the consequence of formation and adsorption of iron oxide or hydroxide species on the surface.[66, 67, 69] Therefore, at a certain point, the suspension could become so acidic (because of either prolonged oxidation or arbitrary acidity control) that its pH (e.g., pH < 4) becomes significantly lower than the pH_{iep} of oxidized pyrite. In such cases, the surface of oxidized pyrite should carry positive charges and thus could readily adsorb the negatively charged AuNPs through electrostatic attraction.

We have demonstrated that pyrite can be oxidized under both anoxic and aerobic conditions in our experiments (Figs. 3, 5–7). Under certain conditions (i.e., suitable combination of experimental parameters such as pH, reaction time, particle sizes, etc.), the amount of AuNP sorption on pyrite can be very high or even reach 100% (see Figs. 3 and 8). A thorough analysis of all our data combined with an extensive literature survey leads us to believe that the pH_{iep} of our oxidized pyrite under initially acidic condition falls in the range of 4–5. Therefore, since the initial pH of Au-39 (∼3.9) was lower than the pH_{iep} of our oxidized pyrite, the pyrite samples shown in Figure 3(a) carried positive charges and readily adsorbed negatively charged AuNPs. Meanwhile, since the decline of pH with time (due to continuous pyrite oxidation) suggests increasing positive charges on pyrite surface, the sorption percentages increased with reaction time. Conversely, because the initial pH of Au-16 (∼6.13) was higher than the pH_{iep}, the pyrite samples (Py-134 + Au-16) in Figure 3(b) initially carried negative charges, and did not adsorb AuNPs until after over 2 days of shaking when the system pH was lowered to ∼4. As shown in both Figures 3(a) and (b), a nearly complete sorption of AuNPs was only observed after 6 days of reaction when the pH was further lowered to <3.0, which suggests considerable amount of positive charges on the pyrite samples.

For the sorption samples shown in Figure 8, the initial pHs were intentionally adjusted and their changes were affected by pyrite oxidation under controlled atmosphere. For similar reasons, complete adsorption of AuNPs within 2–3 days was observed for samples with the initial pH of 3.02 and final pH < 3 (see Figs. 6 and 8). Because of the higher oxidation rate (Fig. 7), the final pHs of the aerobic samples with initial pHs of 6.11 and 7.06 declined to 3.10 and 3.20 respectively (Fig. 6), and thus substantial AuNP sorption was observed. In contrast, since the final pHs (5.23 and 6.04; see Fig. 6) of the corresponding anoxic samples remained much higher than the pH_{iep} of our oxidized pyrite, only trivial AuNPs adsorption was detected. Under initially alkaline conditions (pH 10.02), there was a great extent of oxidation (Fig. 7) and the oxidized products (probably iron oxides or hydroxide) might form fine colloid in the bulk solution and even precipitate on the pyrite surface.[33, 58, 66, 70] These oxidized species usually have pH_{iep}'s (e.g., $pH_{iep} \sim 9.3$ for hematite) much higher than the final pH of the suspension (pH 6.85; see Fig. 6), and could thus efficiently adsorb or destabilize AuNPs through heteroaggregation.[71]

It seems straightforward to understand the size effect between Py-134 and Py-242 revealed in Figure 3, as the larger specific surface area associated with Py-134 should promote overall oxidation and sorption processes. The sorption behaviors of Au-16 and Au-39 samples are quite different, and we have already explained the lagging adsorption of Au-16 (Fig. 3(b)) by pointing out that its initial pH (6.13) was higher than the inferred pH_{iep} (4–5) of our oxidized pyrite. We also noticed that at pH < 4, it took 4 days for the bigger Au-39 series to achieve complete adsorption, which is much longer than that (3 days) for the smaller Au-16 series. A possible explanation is that the smaller AuNPs usually carry more surface charges as reflected by the higher negative zeta potentials.[72] On the other hand, to reach the same lowered pH, the extent of pyrite oxidation may be larger in Au-16 because of its relatively higher initial pH, which implies larger amounts of positive charges on pyrite in the Au-16 samples.

We are also aware that S species on pyrite may displace citrate ligand on AuNPs and form a complex S-Au interface.[73] However, such a ligand exchange reaction normally requires overcoming considerable amounts of activation energy due to electrostatic and steric repulsions. Besides, after oxidation, the density of surface S species on pyrite may be significantly reduced. Therefore, we still believe that our electrostatic interaction mechanism is robust enough to explain most experimental findings.

4. CONCLUSIONS

The sorption behavior of AuNPs on the surface of pyrite was systematically investigated. We have found that experimental variables such as atmosphere, pH, and particle sizes all substantially impact the sorption process, and proposed a robust electrostatic model to explain all our experimental findings. Oxidation of pyrite constitutes a vital part in our mechanism, which accounts for the increase

of pyrite's pH_{iep} and the decrease of the suspension pH. Under suitable conditions (i.e., lower system pH, prolonged oxidation time, smaller pyrite size, etc.), pyrite can carry considerable amounts of positive charges and reach complete sorption of negatively charged AuNPs through electrostatic attraction. Our study has emphasized the importance of surface charge property and oxidative conditions in predicting the transport and fate of natural and engineered nanoparticles in the environment, which provides new insights into the diverse and complex nanogeoscience-related research areas including ore deposits, pollution control, etc. The preliminary success of this work also urges further research endeavors aiming at more comprehensive simulation of related natural processes at elevated temperature and pressure conditions.

Acknowledgment: This work is supported by the Chinese Academy of Sciences ("Hundred Talents Program") and the National Natural Science Foundation of China (41173074).

References and Notes

1. R. Hough, R. Noble, and M. Reich, *Ore Geol. Rev.* 42, 55 (**2011**).
2. H. L. Hong, Q. Y. Wang, J. P. Chang, S. R. Liu, and R. Z. Hu, *Can. Mineral.* 37, 1525 (**1999**).
3. C. S. Palenik, S. Utsunomiya, M. Reich, S. E. Kesler, L. M. Wang, and R. C. Ewing, *Am. Mineral.* 89, 1359 (**2004**).
4. M. Reich, S. E. Kesler, S. Utsunomiya, C. S. Palenik, S. L. Chryssoulis, and R. C. Ewing, *Geochim. Cosmochim. Acta* 69, 2781 (**2005**).
5. R. M. Hough, R. R. F. Noble, G. J. Hitchen, R. Hart, S. M. Reddy, M. Saunders, P. Clode, D. Vaughan, J. Lowe, D. J. Gray, R. R. Anand, C. R. M. Butt, and M. Verrall, *Geology* 36, 571 (**2008**).
6. R. M. Hough, C. R. M. Butt, and J. Fischer-Buehner, *Elements* 5, 297 (**2009**).
7. H. L. Hong and L. Y. Tie, *Clays Clay Miner.* 53, 162 (**2005**).
8. W. C. Su, H. T. Zhang, R. Z. Hu, X. Ge, B. Xia, Y. Y. Chen, and C. Zhu, *Miner. Depos.* 47, 653 (**2012**).
9. G. Simon, S. E. Kesler, and S. Chryssoulis, *Econ. Geol.* 94, 405 (**1999**).
10. N. J. Cook, C. L. Ciobanu, and J. W. Mao, *Chem. Geol.* 264, 101 (**2009**).
11. M. Reich, S. Utsunomiya, S. E. Kesler, L. Wang, R. C. Ewing, and U. Becker, *Geology* 34, 1033 (**2006**).
12. G. Simon, H. Huang, J. E. Penner-Hahn, S. E. Kesler, and L. S. Kao, *Am. Mineral.* 84, 1071 (**1999**).
13. M. Reich, R. M. Hough, A. Deditius, S. Utsunomiya, C. L. Ciobanu, and N. J. Cook, *Ore Geol. Rev.* 42, 1 (**2011**).
14. R. J. Herrington and J. J. Wilkinson, *Geology* 21, 539 (**1993**).
15. J. A. Saunders, *Geology* 18, 757 (**1990**).
16. A. Romanchenko, Y. L. Mikhlin, and L. Makhova, *Glass Phys. Chem.* 33, 417 (**2007**).
17. J. L. Muntean, J. S. Cline, A. C. Simon, and A. A. Longo, *Nat. Geosci.* 4, 122 (**2011**).
18. Y. J. Chen, P. Ni, H. R. Fan, F. Pirajno, Y. Lai, W. C. Su, and H. Zhang, *Acta Petrol. Sin* 23, 2085 (**2007**).
19. Q. F. Gu, G. Krauss, W. Steurer, F. Gramm, and A. Cervellino, *Phys. Rev. Lett.* 100, 045502 (**2008**).
20. X. G. Hong, T. S. Duffy, L. Ehm, and D. J. Weidner, *J. Phys.-Condes. Matter.* 27, 485303 (**2015**).
21. C. Frondel, *Econ. Geol.* 33, 1 (**1938**).
22. P. A. Schoenly and J. A. Saunders, *Fractals-Complex Geom. Patterns* 1, 585 (**1993**).
23. J. A. Saunders and P. A. Schoenly, *Miner. Depos.* 30, 199 (**1995**).
24. A. M. Widler and T. M. Seward, *Geochim. Cosmochim. Acta* 66, 383 (**2002**).
25. M. J. Scaini, G. M. Bancroft, and S. W. Knipe, *Am. Mineral.* 83, 316 (**1998**).
26. V. L. Tauson, S. V. Lipko, and Y. V. Shchegolkov, *Crystallogr. Rep.* 54, 1219 (**2009**).
27. Y. Mikhlin and A. Romanchenko, *Geochim. Cosmochim. Acta* 71, 5985 (**2007**).
28. L. M. Maddox, G. M. Bancroft, M. J. Scaini, and J. W. Lorimer, *Am. Mineral.* 83, 1240 (**1998**).
29. J. R. Mycroft, G. M. Bancroft, N. S. McIntyre, and J. W. Lorimer, *Geochim. Cosmochim. Acta* 59, 3351 (**1995**).
30. Y. Mikhlin, A. Romanchenko, M. Likhatski, A. Karacharov, S. Erenburg, and S. Trubina, *Ore Geol. Rev.* 42, 47 (**2011**).
31. M. B. M. Monte, F. F. Lins, and J. F. Oliveira, *Int. J. Miner. Process.* 51, 255 (**1997**).
32. Y. L. Mikhlin, A. S. Romanchenko, and I. P. Asanov, *Geochim. Cosmochim. Acta* 70, 4874 (**2006**).
33. P. Bonnissel-Gissinger, M. Alnot, J. J. Ehrhardt, and P. Behra, *Environ. Sci. Technol.* 32, 2839 (**1998**).
34. A. P. Chandra and A. R. Gerson, *Geochim. Cosmochim. Acta* 75, 6239 (**2011**).
35. A. N. Buckley and R. Woods, *Appl. Surf. Sci.* 27, 437 (**1987**).
36. P. Zhang, S. H. Yuan, and P. Liao, *Geochim. Cosmochim. Acta* 172, 444 (**2016**).
37. I. N. Myagkaya, E. V. Lazareva, M. A. Gustaytis, and S. M. Zhmodik, *J. Geochem. Explor.* 160, 16 (**2016**).
38. B. L. Shcherbov, V. D. Strakhovenko, S. M. Zhmodik, and Y. A. Kalinin, *Geol. Ore Depos.* 47, 155 (**2005**).
39. C. M. Eggleston and M. F. Hochella, *Science* 254, 983 (**1991**).
40. C. M. Eggleston and M. F. Hochella, *Am. Mineral.* 78, 877 (**1993**).
41. M. C. Daniel and D. Astruc, *Chem. Rev.* 104, 293 (**2004**).
42. J. Zacharias, J. Fryda, B. Paterova, and M. Mihaljevic, *Mineral. Mag.* 68, 31 (**2004**).
43. L. Chen, Occurrence and distribution of gold in the Qiuling carlin-type gold deposit, western Qinling orogen, *GSA Annual Meeting*, Minneapolis, China (**2011**).
44. G. Frens, *Nature-Physical Science* 241, 20 (**1973**).
45. M. Descostes, P. Vitorge, and C. Beaucaire, *Geochim. Cosmochim. Acta* 68, 4559 (**2004**).
46. S. Kumar, K. S. Gandhi, and R. Kumar, *Ind. Eng. Chem. Res.* 46, 3128 (**2007**).
47. X. Ji, X. Song, J. Li, Y. Bai, W. Yang, and X. Peng, *J. Am. Chem. Soc.* 129, 13939 (**2007**).
48. A. G. Schaufuss, H. W. Nesbitt, I. Kartio, K. Laajalehto, G. M. Bancroft, and R. Szargan, *Surf. Sci.* 411, 321 (**1998**).
49. V. P. Evangelou and Y. L. Zhang, *Crit. Rev. Environ. Sci. Technol.* 25, 141 (**1995**).
50. S. B. Dehaan, *Earth-Sci. Rev.* 31, 1 (**1991**).
51. J. D. Rimstidt and D. J. Vaughan, *Geochim. Cosmochim. Acta* 67, 873 (**2003**).
52. M. A. A. Schoonen, A. D. Harrington, R. Laffers, and D. R. Strongin, *Geochim. Cosmochim. Acta* 74, 4971 (**2010**).
53. A. P. Chandra and A. R. Gerson, *Surf. Sci. Rep.* 65, 293 (**2010**).
54. P. C. Singer and W. Stumm, *Science* 167, 1121 (**1970**).
55. R. T. Lowson, *Chem. Rev.* 82, 461 (**1982**).
56. E. M. Hotze, T. Phenrat, and G. V. Lowry, *J. Environ. Qual.* 39, 1909 (**2010**).
57. L. Lu, R. C. Wang, J. Y. Xue, F. R. Chen, and J. Chen, *Sci. China, Ser. D* 48, 1690 (**2005**).
58. V. S. T. Ciminelli and K. Osseoasare, *Metall. Mater. Trans. B-Proc. Metall. Mater. Proc. Sci.* 26, 677 (**1995**).
59. A. D. Brown and J. J. Jurinak, *Arid Soil Res. Rehab.* 3, 65 (**1989**).

60. G. W. Luther, The frontier-molecular-orbital theory approach in geotechnical processes, Aquatic Chemical Kinetics, edited by W. Stumm, John Wiley & Sons, New York **(1990)**, p. 173.
61. S. Basu, S. K. Ghosh, S. Kundu, S. Panigrahi, S. Praharaj, S. Pande, S. Jana, and T. Pal, *J. Colloid Interface Sci.* 313, 724 **(2007)**.
62. J. F. Liu, S. Legros, G. B. Ma, J. G. C. Veinot, F. von der Kammer, and T. Hofmann, *Chemosphere* 87, 918 **(2012)**.
63. S. H. Brewer, W. R. Glomm, M. C. Johnson, M. K. Knag, and S. Franzen, *Langmuir* 21, 9303 **(2005)**.
64. S. Vijayakumar and S. Ganesan, *Indian J. Phys.* 86, 989 **(2012)**.
65. S. Diegoli, P. M. Mendes, E. R. Baguley, S. J. Leigh, P. Iqbal, Y. R. G. Diaz, S. Begum, K. Critchley, G. D. Hammonds, S. D. Evans, D. Attwood, I. P. Jones, and J. A. Preece, *J. Exp. Nanosci.* 1, 333 **(2006)**.
66. J. Bebie, M. A. A. Schoonen, M. Fuhrmann, and D. R. Strongin, *Geochim. Cosmochim. Acta* 62, 633 **(1998)**.
67. D. Fornasiero, V. Eijt, and J. Ralston, *Colloids and Surfaces* 62, 63 **(1992)**.
68. M. Pontes-Buarque, A. C. Tessis, J. A. P. Bonapace, M. B. M. Monte, F. De Souza-Barros, and A. Vieyra, *An. Acad. Bras. Cienc.* 72, 317 **(2000)**.
69. E. C. Todd, D. M. Sherman, and J. A. Purton, *Geochim. Cosmochim. Acta* 67, 881 **(2003)**.
70. C. L. Caldeira, V. S. T. Ciminelli, A. Dias, and K. Osseo-Asare, *Int. J. Miner. Process.* 72, 373 **(2003)**.
71. B. M. Smith, D. J. Pike, M. O. Kelly, and J. A. Nason, *Environ. Sci. Technol.* 49, 12789 **(2015)**.
72. T. Kim, K. Lee, M.-S. Gong, and S.-W. Joo, *Langmuir* 21, 9524 **(2005)**.
73. E. Pensa, E. Cortes, G. Corthey, P. Carro, C. Vericat, M. H. Fonticelli, G. Benitez, A. A. Rubert, and R. C. Salvarezza, *Acc. Chem. Res.* 45, 1183 **(2012)**.

Received: 12 April 2016. Accepted: 8 November 2016.